Colloidal Nanoparticles of Ln^{3+}-Doped $LaVO_4$: Energy Transfer to Visible- and Near-Infrared-Emitting Lanthanide Ions

Jan W. Stouwdam,[†] Mati Raudsepp,[‡] and Frank C. J. M. van Veggel*,[†]

Laboratories of Supramolecular Chemistry and Technology & MESA+ Research Institute, University of Twente, P.O. Box 217, 7500 AE Enschede, The Netherlands

Received February 25, 2005. In Final Form: May 16, 2005

Colloidal, organic solvent-soluble Ln^{3+}-doped $LaVO_4$ nanoparticles have been synthesized by a precipitation reaction in the presence of $(C_{18}H_{37}O)_2PS_2^-$ as ligand, that coordinates to the surface of the nanoparticles. The materials are well soluble in chlorinated solvent such as chloroform. Energy transfer of excited vanadate groups has been observed for Ln^{3+} ions that emit in the visible and the near-infrared (Eu^{3+}, Tm^{3+}, Nd^{3+}, Er^{3+}, Ho^{3+}, Dy^{3+}, Sm^{3+}, Pr^{3+}), thus making it a very generic sensitization mechanism. The $LaVO_4$ nanoparticles have a different crystal structure than bulk $LaVO_4$ ones (xenotime instead of monazite), similar to YVO_4 nanoparticles. This xenotime crystal structure results in a more asymmetric crystal field around the Ln^{3+} ions that is advantageous to their luminescence, for it increases the radiative rate constant, thus reducing quenching processes.

Introduction

Luminescent nanoparticles that are soluble in organic solvents and polymers attract a great deal of interest, because these materials can easily be processed via spin-coating from organic solution. Solubility is generally achieved by the coordination of a monolayer of (charged) ligands on the surface of the nanoparticles, thus leading to colloidal materials. The focus has mainly been on semiconductor nanoparticles, but an interesting class of materials is the lanthanide-doped nanoparticles. Lanthanide ions doped in the nanoparticles show luminescence properties that are very similar to those of the bulk materials.[1−5] The lanthanide ions in these nanoparticles are shielded from the organic environment, and as a result high quantum yields and long luminescence lifetimes are observed. This is particularly important for Ln^{3+} ions that emit in the near-infrared, because the energy involved in the transitions is smaller, and thus the quenching by OH and to a lesser extent CH groups is much more pronounced. The luminescence of lanthanide ions originates from intra-4f transitions and does not involve valence electrons; as a result, luminescent materials based on lanthanide ions are very stable against photooxidation. The high stability is especially useful for applications that require high pump powers, such as lasers and optical amplifiers. These lanthanide-doped nanoparticles make it possible to study processes that need high laser power excitation in these organic host materials. Haase et al. showed that nanoparticles of $LaPO_4$ and $NaYF_4$ doped with Yb^{3+}, Er^{3+} and Yb^{3+}, Tm^{3+} can show up-conversion in solution.[6,7] We have focused on soluble core and core−shell nanoparticles based on Ln^{3+}-doped LaF_3 and $LaPO_4$ that emit in the near-infrared (NIR).[3−5] Furthermore, we showed that surface modification can be done by ligand-exchange reactions in solution, and in the case of $LaPO_4$, covalent reactions are also possible between the surface phosphate groups and alcohols.[8] Ligand-exchange reactions in solution are usually fast and quantitative if the new ligand binds more strongly to the surface than the original. In our group we showed that nanoparticles of LaF_3 doped with Nd^{3+} can be used in polymer waveguide amplifiers that operate in the 1.33 μm band of the telecommunication window.[9] A recent publication by us discusses the optical properties of surface versus "bulk" Eu^{3+} ions in colloidal nanoparticles through a systematic study of Eu^{3+} concentration, ligand-exchange reactions, and core and core−shell nanoparticles.[10]

The direct excitation of the lanthanide ions is a relatively inefficient process, due to the forbidden character of the 4f transitions (extinction coefficient are typically 1−10 M^{-1} cm^{-1}). Energy transfer from a host material or other ion with a higher absorption coefficient could lead to much more efficient materials. Eu^{3+} and Yb^{3+} ions doped in the $LaPO_4$ nanoparticles can be excited using a charge-transfer transition in the Ln−O bond, because Eu^{2+} and Yb^{2+} are stable oxidation states. Tb^{3+} ions can be excited using energy transfer from excited co-doped Ce^{3+} ions, which have an allowed 4f−5d absorption in the UV. This sensitization with Ce^{3+} is only efficient with Tb^{3+}, not markedly efficient with Sm^{3+} and Dy^{3+}, and not effective with Eu^{3+}, the latter probably because of redox processes. LaF_3 nanoparticles doped with Ln^{3+} ions can, in general,

[†] Current address: Department of Chemistry, University of Victoria, P.O. Box 3065, Victoria BC, Canada V8W 3V6. E-mail: fvv@uvic.ca.

[‡] Department of Earth & Ocean Sciences, University of British Columbia, Vancouver BC, Canada V6T 1Z4.

(1) Riwotzki, K.; Meyssamy, H.; Schnablegger, H.; Kornowski, A.; Haase, M. *Angew. Chem., Int. Ed.* **2001**, *40*, 573.

(2) Riwotzki, K.; Meyssamy, H.; Kornowski, A.; Haase, M. *J. Phys. Chem. B* **2000**, *104*, 2824.

(3) Stouwdam, J. W.; Hebbink, G. A.; Huskens, J.; van Veggel, F. C. J. M. *Chem. Mater.* **2003**, *15*, 4604.

(4) Hebbink, G. A.; Stouwdam, J. W.; Reinhoudt, D. N.; van Veggel, F. C. J. M. *Adv. Mater.* **2002**, *14*, 1147.

(5) Stouwdam, J. W.; van Veggel, F. C. J. M. *Nano Lett.* **2002**, *2*, 733.

(6) Heer, S.; Lehmann, O.; Haase, M.; Güdel, H. U. *Angew. Chem., Int. Ed.* **2003**, *42*, 3179.

(7) Heer, S.; Kömpe, K.; Güdel, H. U.; Haase, M *Adv. Mater.* **2004**, *16*, 2102.

(8) Stouwdam, J. W.; van Veggel, F. C. J. M. *Langmuir* **2004**, *20*, 11763.

(9) Dekker, R.; Klunder, D. J. W.; Borreman, A.; Diemeer, M. B. J.; Wörhoff, K.; Driessen, A.; Stouwdam, J. W.; van Veggel, F. C. J. M. *Appl. Phys. Lett.* **2004**, *85*, 6104.

(10) Sudarsan, V.; van Veggel, F. C. J. M.; Herring, R. A.; Raudsepp, M. *J. Mater. Chem.* **2005**, *15*, 1332.

10.1021/la0505162 CCC: $30.25
Published on Web 06/23/2005

only be excited via direct excitation of the Ln^{3+} ions. However, Yb^{3+} can be used as sensitizer of Er^{3+}; nevertheless, even though Yb^{3+} is more efficient than direct Er^{3+} excitation, the extinction coefficient of Yb^{3+} is still low.[3] Therefore, it would be advantageous to have a more general and more efficient approach to excite the other lanthanide ions as well. Doping of lanthanide ions in semiconductor nanoparticles is a possible option, but it proved difficult to dope the lanthanide ion in the nanoparticle cores of several of these materials.[11] We did report the successful doping of lanthanide ions in TiO_2 nanoparticles and showed that energy transfer between the semiconductor host to several lanthanide ions takes place, but the quantum yields of these materials were low.[12]

With direct excitation being rather inefficient and energy transfer from excited Ce^{3+} working well for Tb^{3+} only and the charge-transfer band involving oxygen only operable with Eu^{3+} and Yb^{3+}, there is a clear need to have general excitation methods for the luminescent Ln^{3+} ions, in particular the ones that emit in the NIR. Procedures to synthesize lanthanide-doped YVO_4 nanoparticles in *aqueous* solution have been described, in which the energy transfer from excited VO_4 groups is being exploited.[13−17] Most of these efforts focus on Eu^{3+}; the only other lanthanide ions that were used were the visible-emitting ions Dy^{3+} and Sm^{3+}.[16] In this paper we describe the synthesis of $LaVO_4$ nanoparticles that are soluble in organic solvents, through the coordination of negatively charged ligands on the surface of the nanoparticles. These nanoparticles provide the possibility to excite most of the lanthanide ions via the charge-transfer transition within the vanadate group, followed by energy transfer to the emissive Ln^{3+}. They offer a unique crystal site to the doping ion with very low symmetry, which increases the radiative rate constant, thus giving quenching processes less chance.

Experimental Section

General. TEM images were collected on a Philips CM 30 Twin FTEM, operating at 300 kV. Samples were prepared by evaporating a drop of a diluted nanoparticle dispersion in dichloromethane on a carbon-coated 200 mesh copper grid. X-ray fluorescence was carried out on a Philips PW 1489 spectrometer using LaF_3, Li_3PO_4, and Eu_2O_3 as the standards. Elemental analyses were performed on a Carlo Erba EA 1106 apparatus. For the XRD measurements approximately 40−50 mg of a sample was gently stirred in an alumina mortar to break up lumps. The powder was subsequently smeared on to a zero-diffraction quartz plate using ethanol. Step-scan X-ray powder-diffraction data were collected over the 2θ range 3−100° with Cu Kα (40 kV, 40 mA) radiation on a Siemens D5000 Bragg−Brentano $\theta-2\theta$ diffractometer equipped with a diffracted-beam graphite monochromator crystal, 2 mm (1°) divergence and anti-scatter slits, 0.6 mm receiving slit, and incident beam Soller slit. The scanning step size was 0.04° 2θ with a counting time of 2 s/step. Data are presented from $2\theta = 12-100°$, because there are no features below 12°. The X-ray powder diffraction pattern of $LaVO_4$ was refined in space group $D^{19}{}_{4h}$ with the Rietveld program Topas 3.0 (Bruker AXS 2003)[18] using the fundamental parameters approach (Cheary and Coelho, 1992).[19]

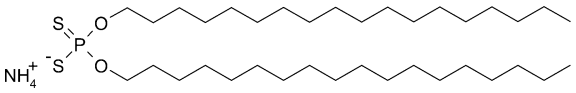

1

Figure 1. Dithiophosphate ligand used in the synthesis of $LaVO_4$:Ln nanoparticles.

The lanthanide salts were purchased from Aldrich or Acros in the highest purity available (at least 99.9%). All chemicals were used as received without further purification. CH_2Cl_2 and hexane were distilled from $CaCl_2$, ethyl acetate was distilled from K_2CO_3.

Ln^{3+}-Doped $LaVO_4$ Nanoparticles. The ligand was synthesized as reported previously.[3] The $LaVO_4$ nanoparticles were prepared by heating a solution of 0.95 mmol ligand **1** (618 mg) and 184 mg (1 mmol) sodium orthovanadate in 35 mL of ethanol/water at 75 °C. A solution of $La(NO_3)_3{\cdot}6H_2O$ and $Ln(NO_3)_3{\cdot}6H_2O$ (1.33 mmol total of which 5 mol % was of the luminescent ion, unless otherwise stated) in 2 mL of water was added dropwise, and the solution was stirred at 75 °C for 2 h and then cooled to room temperature. The precipitate was separated by centrifugation and was washed subsequently with water and ethanol. The nanoparticles were further purified by dispersing in 2 mL of dichloromethane and precipitating by the addition of 20 mL of ethanol. After separation by centrifugation the nanoparticles were dried in a vacuum over P_2O_5 for 2 days. After drying, the nanoparticles are soluble in apolar solvents such as chloroform, dichloromethane, and toluene.

Methods. Photoluminescence measurements in the visible were done with an Edinburgh Instruments FS/FL instrument with a 450 W Xe arc lamp, and for the time-resolved measurements, a micro-flashlamp as the excitation source. The excitation light was fed to a monochromator (single grating, 1800 lines/mm) and focused on a square quartz cuvette (1×1 cm^2) containing the nanoparticle solution. The emitted visible light was fed to a second monochromator (1800 lines/mm grating) and collected on a red-sensitive Peltier element cooled Hamamatsu R955 PMT. The emission spectra were corrected for the detector response, and the excitation spectra were corrected for the lamp intensity. The NIR spectra were measured with the same instrument using a liquid nitrogen-cooled Ge detector and a monochromator equipped with a 600 lines/mm grating. The luminescence lifetime of Nd^{3+} was measured using a liquid nitrogen-cooled Hamamatsu R5509 NIR-PMT. Luminescence quantum yields were determined by comparing the luminescence intensity of a particle solution with a solution of quinine bisulfate in 1 M H_2SO_4 with approximately the same absorption at the excitation wavelength, taking the quantum yield of quinine bisulfate as 54.4%.[20]

Results and Discussion

The synthesis of these $LaVO_4$ nanoparticles is very similar to a procedure described earlier for LaF_3 nanoparticles.[5] This procedure involves the precipitation of the lanthanide salts and vanadate ions in the presence of a dithiophosphate ligand (Ligand **1**) shown in Figure 1. In other words, the process can be characterized as an arrested precipitation because of the presence of ligands that coordinate to the surface of the nanoparticles.

This ligand is present to control the growth of the nanocrystalline particles and to give the nanoparticles solubility in organic solution after their synthesis. Using the same procedure, YVO_4 nanoparticles could also be made, but the dispersibility of these particles was much lower. This is probably a result of increased Ln^{3+}−ligand interaction of the smaller Y^{3+} ion compared to that of La^{3+}.

(11) Bol, A. A.; van Beek, R.; Meijerink, A. *Chem. Mater.* **2002**, *14*, 1121.
(12) Stouwdam, J. W.; van Veggel, F. C. J. M. *ChemPhysChem* **2004**, *5*, 743.
(13) Huignard, A.; Gacoin, T.; Boilot, J. P. *Chem. Mater.* **2000**, *12*, 1090.
(14) Huignard, A.; Buisette, V.; Laurent, G.; Gacoin, T.; Boilot, J. P. *Chem. Mater.* **2002**, *14*, 2264.
(15) Huignard, A.; Buissette, V.; Franville, A. C.; Gacoin, T.; Boilot, J. P. *J. Phys. Chem.* **2003**, *107*, 6754.
(16) Riwotzki, K.; Haase, M. *J. Phys. Chem. B* **1998**, *102*, 10129.
(17) Riwotzki, K.; Haase, M. *J. Phys. Chem. B* **2001**, *105*, 12709.
(18) Bruker AXS 2003: TOPAS V3.0: General profile and structure analysis software for powder diffraction data. User's Manual; Bruker AXS: Karlsruhe, Germany, 2003.
(19) Cheary, R. W.; Coelho, A. A. *J. Appl. Crystallogr.* **1992**, *25*, 109−121.
(20) Eaton, D. F. *Pure Appl. Chem.* **1988**, *60*, 1107.

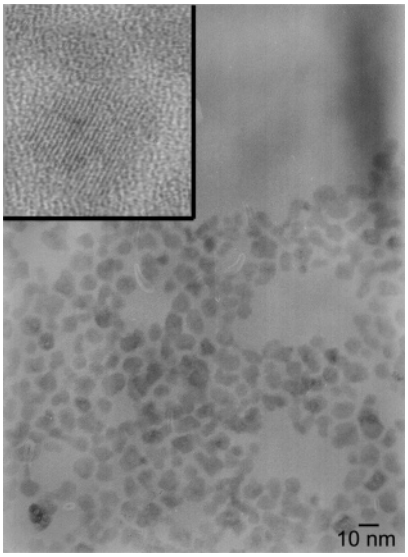

Figure 2. TEM picture of $LaVO_4$:Eu nanoparticles.

Table 1. Elemental Composition of $LaVO_4$:Eu Nanoparticles (wt %)

particle	La[a]	Eu[a]	P[a]	V[a]	C[b]	H[b]	S[b]
$LaVO_4$:Eu	18.46	1.17	4.48	9.24	44.62	7.88	6.70

[a] Measured with XRF. [b] Measured with combustion elemental analysis.

A similar problem was observed previously by us in the synthesis of YF_3 nanoparticles.

A typical transmission electron micrograph (TEM) picture of the $LaVO_4$:Eu nanoparticles is shown in Figure 2.

This TEM picture shows particles with a size between 6 and 10 nm of mostly irregular shapes. The lattice fringes are clearly visible in the magnification of a single nanoparticle, demonstrating the high crystallinity of these nanoparticles.

The elemental composition of the nanoparticles was determined using X-ray fluorescence and combustion elemental analysis. The results of these measurements are summarized in Table 1.

It can be seen that the ratio of lanthanide ions that is found in the nanoparticles is very similar to the ratio applied in the synthesis. This is consistent with a homogeneous, i.e. completely statistical, doping in the nanoparticles. We have shown this in detail in a recent paper.[10] The organic ligand makes up a large part of the total weight. Figure 3 shows the X-ray diffraction (XRD) pattern of $LaVO_4$:Eu nanoparticles.

The X-ray powder diffraction pattern of $LaVO_4$ was refined in space group D^{19}_{4h} with the Rietveld refinement method[18] using the fundamental parameters approach.[19] The pattern fits well with the xenotime structure of $LaVO_4$, in contrast to the monazite structure that is generally observed for bulk $LaVO_4$. This different crystal structure of this nanomaterial was observed before for a nanocrystalline $LaVO_4$ material.[21] The difference in crystal structure between the nanocrystalline $LaVO_4$ and bulk $LaVO_4$ is most likely a result of the increased amount of surface ions in these materials. The crystallite size obtained from the line width of the XRD pattern is 7.9(3) nm, which corresponds well with the sizes that were measured from the TEM micrographs. The unit cell volume of 362.3(1) $Å^3$ is in agreement with the 5% doping level of the smaller Eu^{3+} compared to that of La^{3+}. This decrease in unit cell volume is another good indication that the doping ions are homogeneously distributed in the nanoparticles.[10] The XRD pattern of Pr^{3+}-doped $LaVO_4$ nanoparticles was measured as well (Figure S1, Supporting Information) and gave a very similar result with a slight increase in the lattice parameters, which is in agreement with the larger size of this ion compared to that of Eu^{3+}. To the dopant lanthanide ions, the tetragonal crystal structure offers a crystal site with a D^{19}_{4h} space group (the same as in bulk YVO_4) which has very low inversion symmetry. As a result, electric dipole transitions are more allowed, which results in a higher intensity of the electric dipole transitions, compared to magnetic dipole transitions and hence shorter radiative lifetimes, compared to crystal sites with a higher symmetry. YVO_4 is a well-known crystalline material in which this effect is being utilized. The vanadate groups have a charge-transfer transition in the V−O bond, and it is known that the energy absorbed in this bond can be transferred with high efficiency to Eu^{3+} ions. The absorption coefficient of the vanadate charge-transfer transition is several orders of magnitude higher than that of the lanthanide 4f transitions. It should be possible to transfer this energy to most other lanthanide ions as well, because most of the other luminescent lanthanide ions have energy levels high enough to accept this energy. YVO_4 has a xenotime crystal structure,[22] which offers the Y^{3+} ions a crystal site with D^{19}_{4h} symmetry. Luminescent lanthanide ions doped in the crystal will replace Y^{3+} ions, which gives the luminescent ions a site without inversion symmetry. This lack of inversion symmetry has a significant advantage on the optical properties of the lanthanide ions. In general the lack of inversion symmetry around the lanthanide ions makes the electric dipole transitions more allowed than in a site with inversion symmetry; as a consequence, the rates of absorption and emission are higher, resulting in higher absorption coefficients and higher radiative rates. The higher radiative rates reduce the probability of quenching, which can result in higher quantum yields.

An example where this crystal structure is advantageous is the well-known red-emitting phosphor, YVO_4:Eu. Due to the lack of inversion symmetry around the Eu^{3+} ion, most of the emission is in the hypersensitive $^5D_0 \rightarrow {}^7F_2$ electric dipole transition at 617 nm, which gives the material an intense red emission. Eu^{3+} materials that show emission primarily in the $^5D_0 \rightarrow {}^7F_2$ transition are especially useful for display applications.

YVO_4:Nd is another example. This material is being studied widely for use in high-power solid-state lasers.[23] The absorption coefficient of the Nd^{3+} ion is about 8 times higher than in the often used YAG crystal, which could lead to much more efficient lasers. This difference in absorption strength is mainly caused by the difference in symmetry around the lanthanide ion.

The increase in the electric dipole transition is demonstrated in the emission spectrum of, for instance, the Eu^{3+} ion. The luminescence spectrum of $LaVO_4$:Eu nanoparticles shown in Figure 4 clearly shows the dominating peak at 617 nm of the $^5D_0 \rightarrow {}^7F_2$ electric dipole transition.

The similarity of this emission spectrum with the emission spectra found for bulk YVO_4:Eu confirms that the crystal structure of these $LaVO_4$ nanoparticles

(21) Jia, C. J.; Sun, L. D.; Luo, F.; Jiang, X. C.; Wei, L. H.; Yan, C. H. *Appl. Phys. Lett.* **2004**, *84*, 5305.

(22) Curelaru, I. M.; Suoninen, E.; Ahlqvist, P.; Apell, P.; Minni, E.; Rönnhult, T.; Strid, K. G. *Phys. Rev. B* **1980**, *22*, 4698.

(23) Barnes, N. P.; Storm, M. E.; Cross, P. L.; Skolaut, M. W. *IEEE J. Quantum Electron.* **1990**, *26*, 558.

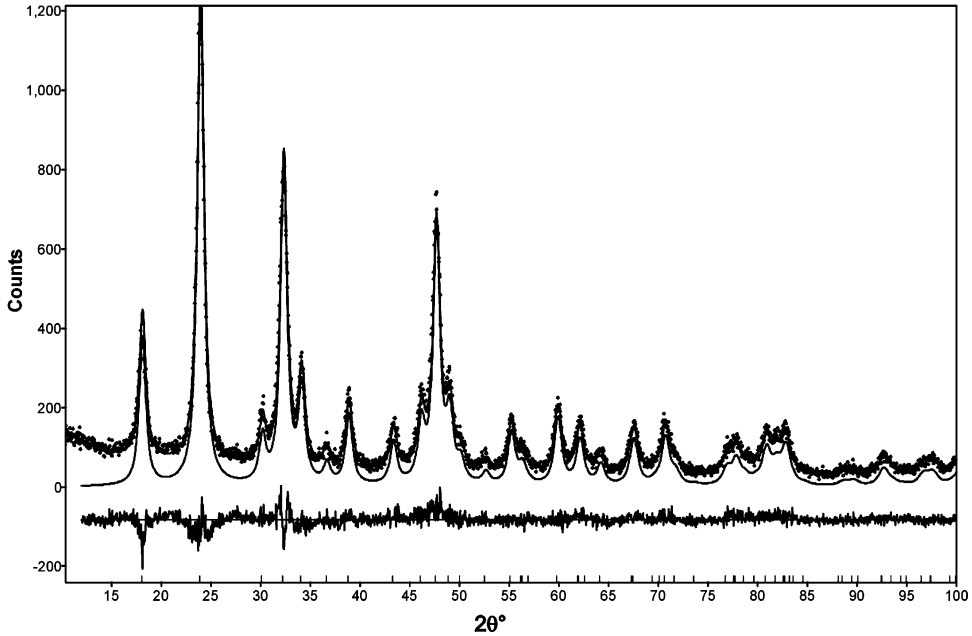

Figure 3. Rietveld refinement plot of $LaVO_4$:Eu nanoparticles (circles, observed pattern; solid line through circles, calculated pattern; solid line below pattern, background subtracted calculated pattern; solid line at bottom, difference curve).

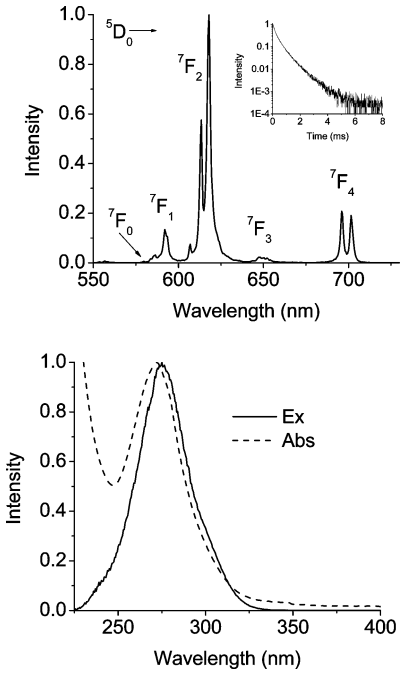

Figure 4. (Top) Emission spectrum ($\lambda_{ex.}$ 280 nm) of $LaVO_4$:Eu nanoparticles in dichloromethane solution. (Inset) Luminescence decay ($\lambda_{ex.}$ 280 nm, λ_{em} 617 nm). (Bottom) Excitation (λ_{em} 617 nm) and absorption spectrum of $LaVO_4$:Eu nanoparticles in dichloromethane solution.

is tetragonal instead of the usual monazite phase.[24] This has clear advantages for some applications such as displays, because most of the Eu^{3+} light is at 617 nm, which gives this material an intense red emission color. A high radiative rate is desirable for displays etc. because it would lead to more photocycles per second and thus to a brighter color. Bulk YVO_4:Eu has been used as the red phosphor in display applications for a long time, because of the good emission properties. The broad absorption band of the VO_4 groups can be seen

(24) Rambabu, U.; Amalnerkar, D. P.; Kale, B. B.; Buddhudu, S. *Mater. Res. Bull.* **2000**, *35*, 929.

Table 2. Quantum Yields of $LaVO_4$:Eu Nanoparticles Doped with Different Concentrations of Eu^{3+}

Eu^{3+} content	quantum yield (%)
5	3.4
10	5.6
15	7.0

in both the excitation spectrum and the absorption spectrum. The excitation spectrum is recorded by scanning the excitation wavelength at a fixed emission wavelength and thus recording those absorptions that lead to a specific emission. The absorption is caused by a charge-transfer transition in the V−O bond, and the energy is subsequently transferred to the Eu^{3+} ion, as expected. The absorption spectrum shows an additional band below 250 nm due to absorption by the ligand, which does not lead to excited Eu^{3+} ions. At this low nanoparticle concentration the 4f absorption lines of the Eu^{3+} ion cannot be observed, which shows that the Eu^{3+} ions are only excited through energy transfer from the vanadate groups.

The inset of Figure 4 shows the luminescence decay. The luminescence lifetimes were fitted using a biexponential decay, and lifetimes of 670 μs (59%) and 190 μs (41%) were obtained. A multiexponential decay is generally observed in these nanoparticles, which can be attributed to an increased chance of quenching of Eu^{3+} ions close to or at the surface of the nanoparticle by the organic ligand and/or coordinated water. These lifetimes are significantly shorter than the lifetimes measured for LaF_3:Eu and $LaPO_4$ nanoparticles synthesized with similar procedures, which is a direct result of the increase in the radiative rates due to the reduced symmetry around the Eu^{3+} ion. For a more eleborate model that describes the decay please refer to our previous work.[3,10]

The quantum yield of these $LaVO_4$:Eu nanoparticles with different concentrations of Eu^{3+} ions was determined by comparing the emission intensity with the emission intensity of quinine bisulfate with the same absorption at the excitation wavelength of 280 nm. The results are summarized in Table 2.

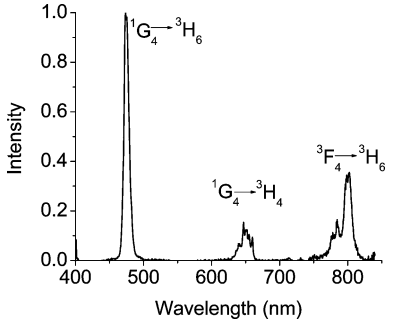

Figure 5. Luminescence spectrum (λ_{ex} 280 nm) of $LaVO_4$:Tm nanoparticles in dichloromethane solution.

The quantum yield at 5% doping level is clearly lower than the quantum yield of 70% of bulk YVO_4.[25] The decreased quantum yield can be a result of increased quenching due to the small particles size or due to a reduced efficiency of energy transfer in the $LaVO_4$ host. The larger size of the La^{3+} ion compared to that of the Y^{3+} ion increases the distance between adjacent vanadate groups, and this could lead to a reduced efficiency of the energy-transfer processes. It can be seen that the quantum yield increases with increasing Eu^{3+} concentration. For the bulk YVO_4:Eu phosphor the maximum quantum yield is observed at a Eu^{3+} concentration of 5%.[16] The quantum yield of this material is determined by how effective the energy transfer of the vanadate groups to the Eu^{3+} ion is; therefore, a higher concentration of Eu^{3+} would lead to a higher quantum yield, but high concentrations of Eu^{3+} lead to self quenching of the Eu^{3+} ions by cross relaxation. These counteracting processes lead to an optimum Eu^{3+} concentration of 5% for the bulk material. Quenching of surface vanadate groups is generally observed in nanocrystals of YVO_4; as a result, the optimum Eu^{3+} can be as high as 15%, and the quantum yield of 70% of the bulk material is not observed.[14] Probably the same applies to our $LaVO_4$:Eu nanoparticles, which leads us to conclude that quenching of surface vanadate groups is an important quenching path in our materials. The synthesis of core−shell structures, in which a layer of inert inorganic material is grown over the $LaVO_4$ core, could prevent most of this surface quenching. Improved optical properties have been shown for LaF_3 and $LaPO_4$ core−shell nanoparticles.[8,10,26] A possible shell material could be $LaPO_4$ that has similar lattice parameters, for it would allow an epitaxial growth of the shell on the surface of the core. An epitaxial growth generally requires that the lattice mismatch of the two materials is usually not larger that a few percent.

Emission of most other luminescent lanthanide ions could also be observed after excitation in the charge-transfer band of the vanadate group, which is demonstrated in Figure 5 with the emission spectrum of $LaVO_4$:Tm.

These nanoparticles emit intense blue light, which is clearly visible under irradiation with a hand-held UV lamp. The blue emission originates from the $^1G_4 \rightarrow {}^3H_6$ transition, but emissions from the $^1G_4 \rightarrow {}^3H_4$ and $^3F_4 \rightarrow {}^3H_6$ transitions at 650 and 790 nm, respectively, are also observed. Emission spectra of other visible-emitting lanthanide ions, such as Dy^{3+}, Pr^{3+}, Sm^{3+}, and Ho^{3+} all excited at 280 nm, can be found in the Supporting Information. All excitation spectra are very similar to the excitation spectrum of the Eu^{3+} ion shown in Figure 4, which demonstrates that energy transfer from the vanadate host to all these ions is also possible.

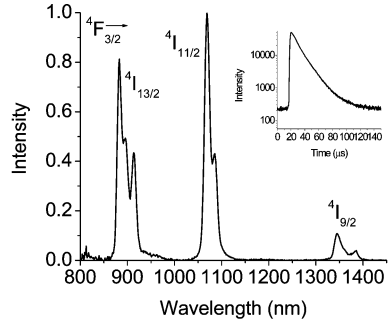

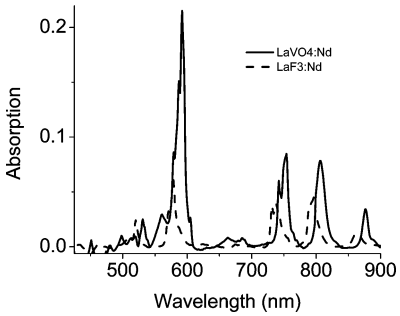

Figure 6. (Top) Emission spectrum of $LaVO_4$:Nd ($\lambda_{ex.}$ 280 nm) in chloroform solution. (Bottom) Baseline-corrected absorption spectra of $LaVO_4$:Nd and LaF_3:Nd nanoparticle solution in chloroform. The Nd^{3+} concentration in both samples is the same.

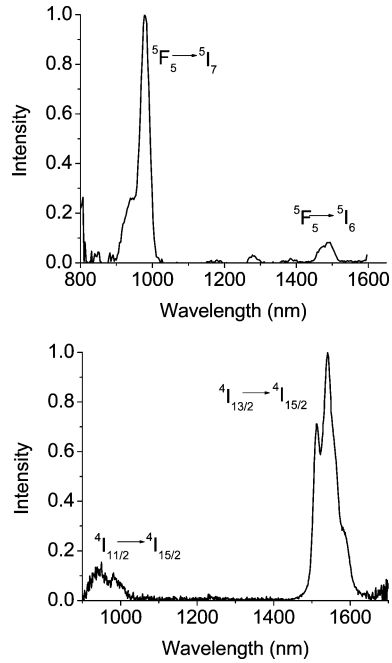

Figure 7. (Top) Emission spectra of $LaVO_4$: Er ($\lambda_{ex.}$ 280 nm) in chloroform solution and (bottom) $LaVO_4$:Ho ($\lambda_{ex.}$ 280 nm) in chloroform solution.

Several NIR-emitting lanthanide ions could also be excited using the charge-transfer band of the VO_4 group. Figure 6 shows the emission spectrum of $LaVO_4$:Nd nanoparticles after excitation at 280 nm.

The emission spectrum shows the typical emissions of Nd^{3+} ion at 880, 1060, and 1330 nm of the transitions from the $^4F_{3/2}$ level to the $^4I_{13/2}$, $^4I_{11/2}$, and $^4I_{9/2}$ levels, respectively. The inset of Figure 6 shows the luminescence

(25) Ropp, R. C. *Luminscence in the Solid State*; Elsevier: Amsterdam, The Netherlands, 1991.

(26) Kömpe, K.; Borchert, H.; Storz, J.; Lobo, A.; Adam, S.; Möller, T.; Haase, M. *Angew. Chem., Int. Ed.* **2003**, *42*, 5513.

decay. The lifetimes could be fitted using a biexponential decay, and lifetimes of 6.2 (21%) and 14.6 (79%) μs were found. The bottom of Figure 6 shows a comparison of the absorption spectra of $LaVO_4$:Nd nanoparticles and LaF_3:Nd nanoparticles with identical Nd^{3+} ion concentrations. It can be seen that the absorption of the Nd^{3+} ions in the $LaVO_4$ host are a little red-shifted and in general much stronger than the absorptions of the Nd^{3+} ion in the LaF_3 host. This could have significant advantages in applications such as lasers and optical amplifiers, in which the lanthanide ions are excited directly, for instance, with diode lasers.

The NIR emission spectra of Er^{3+} and Ho^{3+} after excitation of the VO_4 absorption band are shown in Figure 7.

These spectra show the typical emissions of the Er^{3+} ion at 980 and 1530 nm from the $^4I_{11/2}$ to the $^4I_{15/2}$ transition and the $^4I_{13/2}$ to the $^4I_{15/2}$ transition, respectively, and the emissions of Ho^{3+} at 960 and 1460 nm from the $^5F_5$ level to the $^5I_7$ and $^5I_6$ level, respectively.

Conclusions

The emission properties of colloidal lanthanide-doped nanoparticles that are soluble in organic solvents are mainly determined by the crystal properties of the host material. The possibility to make nanoparticles of different crystal structures is therefore very important for tuning the luminescent properties of these kind of materials. Energy transfer of excited vanadate groups in Ln^{3+}-doped $LaVO_4$ nanoparticles has been demonstrated for visible- and NIR-emitting Ln^{3+} ions, thus making it a generic sensitized emission mechanism. The $LaVO_4$ nanoparticles reported in this work show a different crystal structure than that of the bulk material, and as a result not all the knowledge of bulk crystalline materials can be applied directly to this class of nanocrystalline materials.

Acknowledgment. NWO-CW (The Netherlands) is gratefully acknowledged for financial support of the majority of the work. NSERC (Canada) is acknowledged for the financial support of a small part of this research. CFI and BCKDF (Canada) are acknowledged for financial support of the infrastructure.

Supporting Information Available: Additional figures. This material is available free of charge via the Internet at http://pubs.acs.org.

LA0505162